Enhanced Bus Front End Geometries for Improved Pedestrian Crashworthiness

Phil S. Martin, Jack A. Radcliffe, Muhammad Qasim, Ianto J. Guy

Abstract The influence of the global geometry of bus front ends on pedestrian head and thorax injuries and run-over risks was assessed via computational simulations (LS_DYNA). A concept design, derived from a Design of Experiments (DOE) study, was compared to two existing buses, representing current and previous generation London bus designs. The DOE demonstrated that, when weighted based on London collision data, the risks of head and thorax injuries and run-overs may be minimised by an enhanced bus front end design with a vertical rake angle of 7°, a rake angle transition height of 753 mm and inner and outer horizontal angles of 16° and 24°. When compared to current and previous generation bus front end designs across a range of impact positions, the enhanced bus front end design reduced mean serious (AIS3+) head injury risks by 26-37 percentage points (pp) at 30 mph impact speeds, mean serious (AIS3+) thorax injury risks by 4-5 pp at 20 mph and 30 mph impact speeds and the proportion of run-over events by 20-33 pp at impact speeds <30 mph. This research indicates that substantial casualty saving benefits may be gained with greater consideration given to the global geometry of bus front end designs.

Keywords Bus crashworthiness, pedestrian, head injury, thorax injury, simulation.

I. INTRODUCTION

Pedestrian collisions with buses account for 193 fatalities a year in the EU and form a substantial proportion (31%) of all recorded bus collision related fatalities [1]. In London, it was estimated that 44% of such fatalities suffer a serious head injury, 56% suffer a serious thorax injury and 40% are run-over by the bus [2]. Whilst a range of active and assistive safety measures, such as intelligent speed assistance (ISA), pedestrian and cyclist collision warning systems and driver drowsiness/distraction warning systems, are to be mandated for buses by the new General Safety Regulation (EU) 2019/2144 [3], these will still not be able to prevent all collisions from occurring. Improving the passive safety of bus front ends to improve and optimise protection for pedestrians involved in the remaining collisions therefore remains of considerable societal importance.

Previous research investigating impacts between Heavy Goods Vehicles (HGVs) and pedestrians have shown that interactions during such collisions may be improved through the optimisation of the geometry of the HGV front end [4-8]. The Advanced PROtection SYStems (APROSYS) project, which ran from 2004-2010, investigated the underlying causes of HGV collisions and crashworthiness and the impact of a range of innovative solutions, including a nose cone geometry concept, on pedestrian and cyclist injury risk during the primary and secondary impact phases [4]. That research found that frangible, vertically raked and horizontally curved HGV front end structures improved collision outcomes such as head injury risk and run-over risk, resulting in recommendations that such protective designs be adopted by European legislation for HGV cab length derogations [9].

Using data collated during the APROSYS project, simulations of VRU collisions with a cone-shaped concept truck and a traditional HGV cab geometry were used to predict a reduction in vulnerable road user (VRU) run-over events [5]. During a series of simulations, 6 year old child, 5% female, 50% male, 95% male and 50% cyclist models were simulated to strike the centre and edge of both vehicles. VRU run-overs were 100% prevented in the nine different collision scenarios investigated with the conceptual HGV, whilst the reference HGV ran over the VRU in 66% of collisions [5].

P. S. Martin is the Head of Biomechanics, J. A. Radcliffe is a Graduate Researcher, I. J. Guy is a Vehicle Safety and Technology Consultant and M. Qasim is a Senior Researcher and at the Transport Research Laboratory in the United Kingdom (corresponding author details: pmartin@trl.co.uk (+44)1344770326).

Building on this analysis, a further 192 pedestrian collisions were simulated to compare run-over risk between an optimised and a traditional HGV front end geometry design [6]. The optimised front end geometry (a curved, tapered and plateaued design) was established by comparing the outcomes between six collision simulations performed for 90 different candidate designs. The performance of the optimised design was then compared to a traditional HGV design by varying the HGV manoeuvre, pedestrian size, pedestrian gait cycle, pedestrian collision angle and pedestrian impact position. A reduction in critical run-over events, from 83.3% of collision simulations for the traditional HGV cab design to 12.5% for the optimised design, was observed to demonstrate a considerable improvement in run-over risks with the optimised front end design [6]. Neither APROSYS study, however, determined the differences in pedestrian injury risks during the primary or secondary impact phases, describing these only in terms of the observed head kinematics.

Opportunities for improving pedestrian crashworthiness have also been explored within the tramway sector, with front end design geometry and energy absorbing characteristics similarly found to reduce pedestrian injury risks [10-12]. Pedestrian head injury risks (head injury criteria (HIC)) in the primary impact phase were observed to reduce with the addition of a padded underrun guard and energy absorbing front trim during simulated 35 kph collisions between two different tram designs and a 50% male Hybrid III computational model [10]. Head injury risk (HIC), thoracic injury risk (thorax trauma index (TTI)) and knee injury risk (lateral bending angle) were further optimised for 15 kph tram collisions with an extended fender design located at the lowest investigated vertical position for adult pedestrians and the highest vertical position for children [11]. Finally, head injury risks during both the primary and secondary impact phases were further investigated for 31 tram collisions at 10 kph, 20 kph and 30 kph with 50% male and six year old child pedestrian dummies [12]. Four existing tram front end designs, two trams with extended front trim panels and one virtual tram front end design were investigated, concluding that windscreen angle, the forward displacement of the front trim panel from the windscreen and the energy absorbing A-pillars may all contribute to reducing pedestrian head injury risks [12]. Although these studies indicate that it is possible to improve pedestrian injury risks through optimising tram front end designs, it is unknown to what extent these solutions may be directly transferrable to bus front end designs.

To date, only one study has assessed injury risks associated with pedestrian bus front end collisions [8]. Via a Design of Experiments (DOE) approach that varied the impact speed, braking delay, pedestrian gait, pedestrian facing direction, bus ground clearance and friction properties, the head injury risks associated with a MAN Lion bus model, alongside two HGV models, were investigated. Primary head injury risks, for all reported head injury criteria, were found to be lower for the bus than the two HGV models. It was reported that this was primarily due to the interaction of the pedestrian with the windscreen, where the shoulder impacted and fractured the glazing first to reduce the stiffness of the material prior to a head impact [8].

It is clear from the current state-of-the-art in tram and HGV front end design geometry optimisation research that pedestrian injury risks (during both the primary and secondary impact) and run-over risks may be reduced through improvements in geometry. No such research has, however, been performed to establish whether bus front ends may be similarly enhanced to improve pedestrian collision outcomes. As current bus designs typically have larger glazed areas at the front and rear-mounted engines, this considerably reduces the number of stiff components located in the pedestrian impact zone and this would be expected to result in different kinematic interactions between buses and pedestrians during collisions. It is therefore important to understand whether these unique features of bus front ends may be similarly enhanced to improve pedestrian collisions outcomes.

Through a Design of Experiments (DOE) approach, this research therefore aimed to parametrically sweep a range of global geometric variables for bus front end designs to assess their impact on head and thorax injury risk and run-over risk and enhance the compatibility of bus front end designs. The safety performance of this enhanced bus front end design was then compared to two existing bus model designs to evaluate the potential casualty saving benefits of implementing such design criteria. It was hypothesised that such an enhanced bus front end design may reduce head injury, thorax injury and run-over risks relative to the current state-of-the-art in bus front end designs.

II. METHODS

The objectives of this research were investigated through a computational simulation approach. This used a Design of Experiments (DOE) approach to parametrically generate a series of bus front end design geometries that were impacted by a pedestrian model across a range of speeds and impact positions to derive an enhanced front end design that minimises head injury, thorax injury and run-over risks. The injury risks associated with this enhanced bus front end was then compared to outcomes from two existing bus front end designs.

Bus model build

Computational models of two existing bus designs were created using manufacturer CAD data and material specifications. These existing bus front end designs are typical in their geometry with respect to bus models produced around a decade ago (referred to as B1) and currently in production today (referred to as B2), with both generations currently in service within the London bus fleet. Previous generation designs (B1) are typified by flat fronted box-shaped front ends with the A-pillars located at the frontal plane of the bus, while current generation designs (B2) are typified by wraparound windscreens that have greater vertical raking and A-pillars that are located rearward of the frontal plane of the bus (Figure 1). Both generations of existing bus front ends were investigated in this study, as it was anticipated that these would differ in terms of VRU compatibility and there was no existing evidence to quantify and understand such differences.

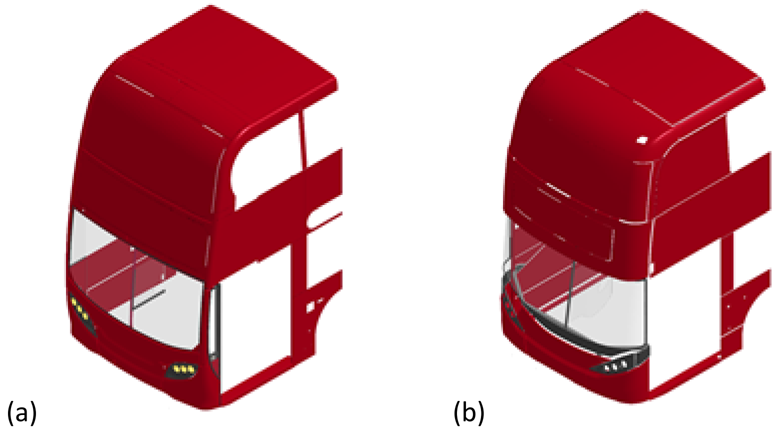

Fig 1. Existing bus front end designs for (a) previous generation (B1) and (b) current generation (B2) models.

A parametric bus model design (referred to as B3) was further developed by morphing the global geometry of the B2 bus model CAD data. The geometric parameters considered for the morphing of the B3 bus front end were the vertical rake, rake transition height, inboard horizontal angle and outboard horizontal angle (Figure 2). The morphing process was used to modify all relevant bus front end components for the B3 model, including all glazing, bodywork and structural elements for the windscreen, A-pillars, bumper and bus superstructure. This ensured that, in addition to morphing the external geometry of the bus, the relevant internal components were also morphed to ensure that any effect of the likely necessary changes in geometry to the stiffer bus front end structures were also accounted for.

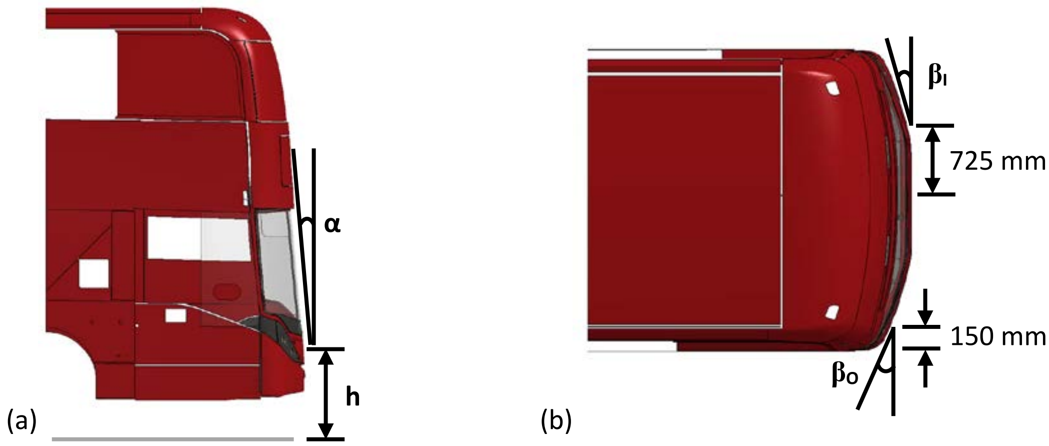

Fig 2. Enhanced B3 bus front end design from (a) side and (b) plan views, illustrating the vertical rake angle (α), rake transition height (h), inboard horizontal angle (β_I) and outboard horizontal angle (β_O) parameters.

Using LS_DYNA PrePost software (version 4.6-x64), the CAD representations of all bus front end models were meshed with fully integrated shell elements (primarily quad shell elements using LS_DYNA element formulation 16 and 5 through-shell thickness integration points to represent geometry thickness). Material properties for each bus front end component, both within and surrounding the pedestrian impact zones, were based on the manufacturer specifications (Table 1), aside from the custom windscreen material model. Material properties were standardised across all three bus models and adopted from the LS_DYNA material model library, whilst all components that were considered to not affect pedestrian collision kinematics were defined as rigid elements.

TABLE 1
LS_DYNA MATERIAL MODELS ADOPTED FOR EACH CATEGORY OF BUS FRONT END COMPONENT

Bus Component	Material	Density /kgm^{-3}	Young's Modulus /GPa	Yield Stress /MPa
Bus Structural Elements	Stainless Steel	7740	200	280
Lower Bumper Bodywork	Polycarbonate-ABS Blend	1120	2.007	20
Upper Bumper Bodywork	Glass Reinforced Plastic	1720	5.5	
Non-Windscreen Glazing	Lexan Margard Polycarbonate	1200	2.35	60
Windscreen Bonding	Adhesive (Elastic)	1000	0.5	

The custom windscreen material model was adopted from a previous study [13] and employed a dual-layer structure constructed of a single shell layer with set thickness for the windscreen glazing material and a second shell layer of polyvinyl butyral plastic (PVB) meshed coincidently over the windscreen layer. The function of the PVB layer was to model the windscreen netting effect during impact by preventing windscreen sections from separating once fractured. The CAD representation of these layers were meshed with 4-node quad elements for the windscreen glazing and PVB shells using LS_DYNA PrePost software (version 4.6-x64), with an average mesh size of 20 mm for all layers.

The windscreen glazing layer adopted an isotropic elasto-plastic material property model, while the PVB layer adopted isotropic hyper-elastic material properties. The material properties of the windscreen glazing and PVB layers were subsequently tuned to correlate with test data from physical headform impact tests [13], which replicated UNECE Regulation 127 adult headform impact tests [14] when performed against the wraparound and flat sections of the B2 windscreen (Figure 3). The tuned material properties for the glazing layer included the density (8775 kg/m^3), Young's modulus (20 GPa), yield stress (55 MPa), tangent modulus (500 MPa) and failure strain (0.005), whilst density (900 kg/m^3) and Young's modulus (20 MPa) were tuned for the PVB layer. Although more complex windscreen material and meshing models could be implemented, the tuned custom windscreen model used in this study provided a reasonable balance between fidelity and computational cost.

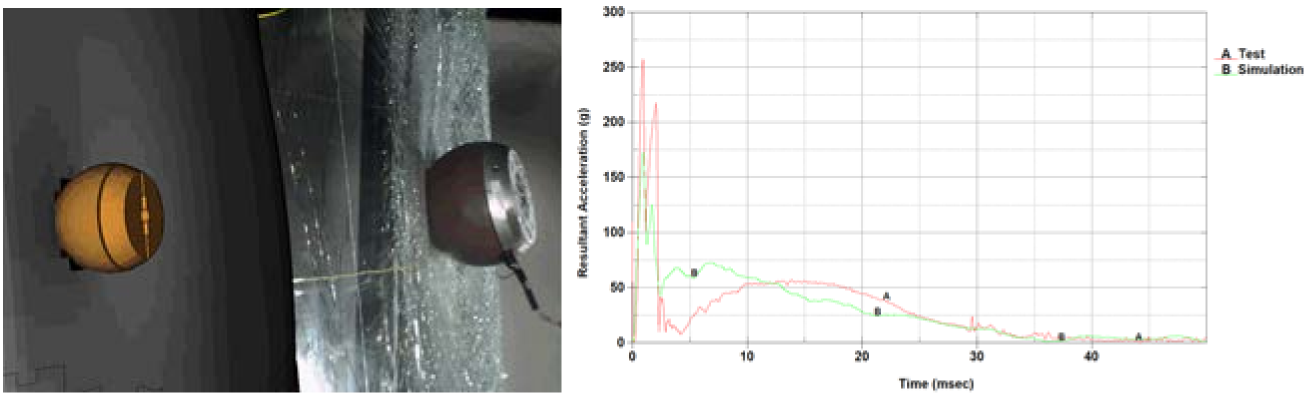

Fig 3. Impact response of custom windscreen model, simulated and tuned to represent analogous test data from [13]. Data shown represents a head impact against the flat section of the windscreen (position 2), with this also tuned to consider impacts against the wraparound section of the windscreen (position 5).

Pedestrian model build

A 50th percentile male pedestrian dummy model, adapted by this study to provide representative side impact responses, was formed by combining a EuroSID-2re (LSTC, v0.201) upper body, neck and head with a Hybrid III FAST (LSTC, v2.0) pelvis and lower limbs. This ensured that the model incorporated a flexible shoulder-thorax complex to better represent the response of the pedestrian when subjected to a side impact, whilst reducing the computational cost of the remaining body regions. The combination of these dummy models also permitted the measurement of both head accelerations and rib deflections during impact. The pedestrian dummy model was positioned such that it adopted a walking posture with its right leg forward and left leg rearward (Figure 4).

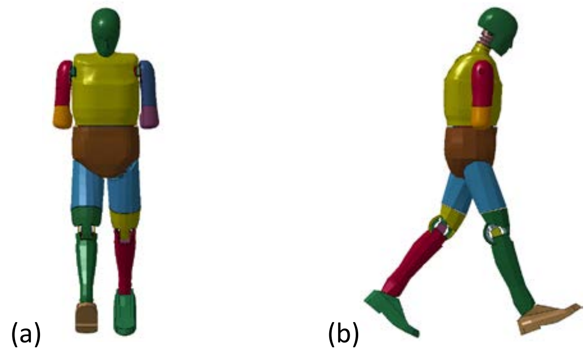

Fig 4. 50th percentile male pedestrian model from (a) front and (b) side views, illustrating pedestrian gait and different body regions.

Collision scenarios

All bus models were located at a consistent height of 325 mm between the bus step and ground plane, which ensures a worst case bus running order height (e.g. maximum tyre pressure, unladen bus, etc.) based on current accessibility requirements in London. All pedestrian models were positioned with 50 mm clearance between the model and the frontal plane of the bus prior to initiation of the simulation. Pedestrian models were located at one of five impact positions across the bus front end (Figure 5), all five of which were found to be associated with fatal pedestrian bus collisions in London [2]. A coefficient of friction of 0.6 between the ground plane and pedestrian was specified, whilst a coefficient of friction of 0.3 was specified between the pedestrian and bus.

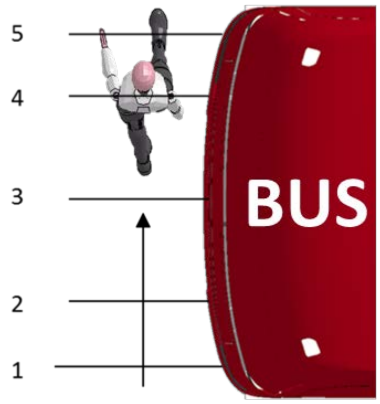

Fig 5. Plan view of the simulated collision scenario showing the five impact positions across the bus front end relative to the pedestrian crossing direction. Positions 1 and 5 are 150 mm from the outer edges, positions 2 and 4 are 725 mm from the centreline of the bus and position 3 is on the centreline of the bus.

Collisions between the pedestrian dummy and bus were simulated using LS_DYNA MPP v8.1.0 finite element analysis software. Bus impact speeds were simulated between 8-32 mph (16.1-48.3 km/h) based on the range of representative collision speeds in fatal pedestrian bus collisions in London [2] and the bus was decelerated at 3.5 m/s^2 to represent realistic peak braking rates achieved by bus drivers in London [15]. During deceleration, the front end was angled forward by 2° to represent the change in angle due to braking dip [15]. Pedestrian models were simulated as crossing from the nearside of the bus to the offside, perpendicular to the direction of travel of the bus, and at a velocity of 4 km/h. This was based on the average walking speed of an adult [16] and the most common crossing direction associated with fatal pedestrian bus collisions in London [2]. In order to reduce computational costs each simulation was run for a total of 250 ms only, thus the injury risks associated with secondary impacts against the ground plane were excluded from this analysis.

Injury risk metrics

Serious head injury, serious thorax injury and run-over risks were calculated for each simulation performed in this study. The probability of an AIS3+ head injury was assessed based on calculating the 15 ms head injury criteria (HIC_{15}) value from the resultant acceleration of the centre of gravity (COG) of the pedestrian head (based on Equation 1) and converting this to an AIS3+ head injury risk probability (based on Equation 2) [17].

$$HIC15 = \max\left[\frac{1}{t_2 - t_1}\int_{t_1}^{t_2} a(t)dt\right]^{2.5} (t_2 - t_1) \quad (1)$$

Where:

a(t) is the resultant head acceleration and $(t_2 - t_1) \leq 15$ milliseconds

$$p(head\ injury) = \varphi\left(\frac{\ln(HIC15) - \mu}{\sigma}\right) \quad (2)$$

Where:

φ is the cumulative normal distribution

μ=7.45231 and σ=0.73998 for AIS3+ head injuries

The probability of an AIS3+ thorax injury was calculated based on the maximum peak rib deflection of the pedestrian model during each simulation (based on Equation 3) [17]. As the EuroSID-2re dummy has three deformable ribs, the maximum peak rib deflection value was recorded from the rib with the greatest deflection during the simulation.

$$p(thorax\ injury) = \frac{1}{1 + e^{(2.0975 - 0.0482 \times max\ rib\ deflection\ )}} \quad (3)$$

Due to the simulation run time limitation of 250 ms, the risk of a run-over event during each simulation was estimated based on extrapolating the trajectory of the pedestrian model from the end of the simulation to the point in time where the bus would come to a halt and assessing whether the bus path would have intersected with the pedestrian trajectory at any point in time. For these estimations, the bus was assumed to be travelling in a straight line and decelerating at a constant rate (i.e. full service braking rate was achieved prior to impact). The estimated trajectory the pedestrian was evaluated in two stages. The first stage estimated the kinematics of the COG of the pedestrian thorax after separation from the bus front end and before impacting the ground, by applying linear equations of motion to the final velocity vector of the thorax COG to calculate the position, time and the velocity vector at the point where the pedestrian would strike the ground. The second stage estimated the kinematics of the thorax COG during an assumed slide event, from the point where the pedestrian would strike the ground to the point at which the sliding motion would cease, based on the deceleration caused by the frictional forces generated between the pedestrian and ground plane.

The separation distance between the frontal plane of the bus and the pedestrian thorax COG was estimated for each collision over time. A run-over event was defined as a minimum separation distance of <0.25 m at any point in time, with each simulation used to establish a binary pass/fail run-over metric (Figure 6). This method of estimating the pedestrian trajectory was validated across four complete impact simulations performed at two pedestrian positions (4 and 5) and two impact speeds (20 mph and 30 mph), which observed acceptable levels for the average and maximum percentage errors in the predicted ground impact position (3.6% and 6.6%) and the predicted final pedestrian sliding position (6.9% and 13.8%).

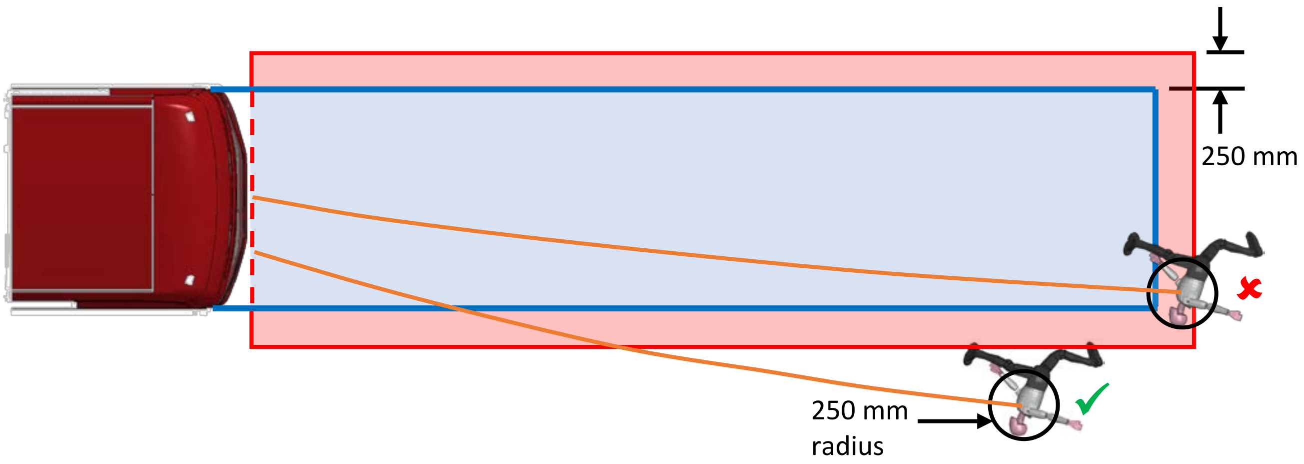

Fig 6. Example trajectory of centre of gravity of the thorax (orange) for the 50th percentile male pedestrian model relative to the vehicle trajectory (blue) and separation distance threshold (red and black circle) during collisions to illustrate the run-over event evaluation (pedestrian assessed as run-over is indicated by a ✖ and pedestrian assessed as thrown clear is indicated by a ✓).

Design of experiments approach

A design of experiments (DOE) approach was used to quantify the combined effects of the four investigated geometric parameters, the five pedestrian impact positions and the bus impact speed using LS-Opt v5.2. A total of 175 simulations were performed based on 35 combinations of bus geometries and impact speeds, matched for each pedestrian impact position. The boundary conditions for the geometric and impact speed parameters investigated by this DOE are shown in Table 2 and were selected following a pilot study to determine the region where the optimum design solution may exist. The geometric parameters were constrained to be as close to the existing flat-fronted bus front end designs as possible, .

A space filling point selection approach was used to generate the 35 selected combinations for each impact position to evenly spread the simulations through the design space and prevent unintentional bias caused by data point clustering. The performance of each design was evaluated against the injury and run-over risk metrics and polynomial (quadratic fit) curves used to determine the DOE response surface for each pedestrian impact position and each injury metric. DOE response surfaces were weighted based on impact speed (<10 mph (22%), 10-20 mph (44%) and >20 mph (33%)) based on data from in-depth investigations of fatal pedestrian bus collisions in London [2]. An enhanced bus front end design solution (B3), which minimised the risks of serious head injuries, thorax injuries and run-overs was then selected based on the DOE response surfaces.

TABLE 2

DESIGN LIMITS FOR DESIGN OF EXPERIMENT

	Minimum Boundary	Maximum Boundary
Inboard Angle	11°	18°
Outboard Angle	20°	33°
Rake Transition Height	750 mm	978 mm
Rake Angle	2°	21°
Vehicle Velocity	8 mph	32 mph

Comparison of bus front end designs approach

The differences in safety performance between existing bus front end designs (B1 and B2) and the enhanced bus front end design (B3) were then compared by simulating pedestrian collisions with each bus front end at all five impact positions (1-5) and three impact speeds (10 mph, 20 mph and 30 mph). Differences in overall safety performance were evaluated by comparing the mean serious head and thorax injury risks and the proportion of predicted run-over events associated with each bus front end design.

III. RESULTS

Design of experiments results

The DOE was used to find the bus front end geometric parameters that gave the best performance across the three injury metrics, five impact positions and all simulated impact velocities. The performance of B2 was used as the benchmark for each of the injury metrics (i.e. B3 was required to have an average performance that was better than B2 for all three metrics), although it was not required to be better than B2 for all possible collision scenarios. The final specification for the enhanced bus front end design is given in Table 3.

TABLE 3
BUS-FRONT GEOMETRY FOR ENHANCED PEDESTRIAN CRASHWORTHINESS

Vertical Rake Angle	Rake Transition Height	Inboard Horizontal Angle	Outboard Horizontal Angle
7°	753 mm	16°	24°

The accuracy of the DOE modelled response surfaces with respect to simulations of specific collision scenarios were found to have R^2>0.96 for the predictions of HIC_{15}, maximum rib deflection and separation distance. All three injury metrics therefore show good agreement between the DOE model predictions and the outcomes of the specific collision simulations.

Comparison of bus front end designs results

The mean percentage serious (AIS3+) head and thorax injury risks resulting for the three different bus designs impacting the 50th percentile male pedestrian model at each impact speed are illustrated in Figure 7. The figure shows that, in general, the probability of an AIS3+ thorax injury is considerably higher for than for a head injury, particularly at impact speeds of 10 mph and 20 mph. A considerable improvement in serious head injury risks was found for each generation of bus front end design at impact speeds of 30 mph, with a substantial reduction for B3 relative to B1 (37 percentage points (pp)) and B2 (26 pp). At lower impact speeds the risks of a serious head injury was less than 6% for all bus front end designs, so the differences in risk were only marginal. Finally, a 4-5 pp reduction in mean AIS3+ thorax injury risk was also found for collisions at 20 mph and 30 mph, when comparing the B3 bus front end design to the B1 and B2 bus front end designs.

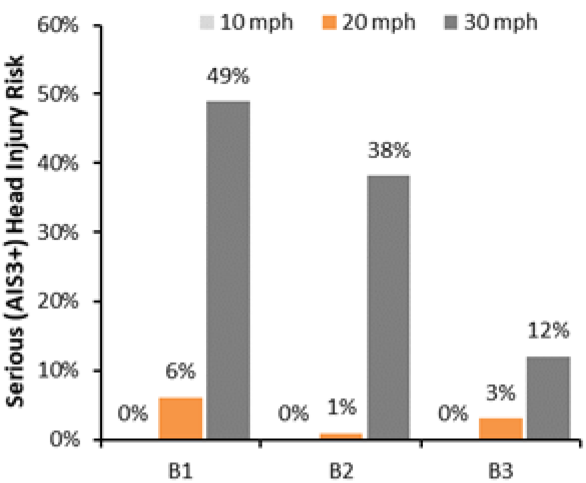

(a)

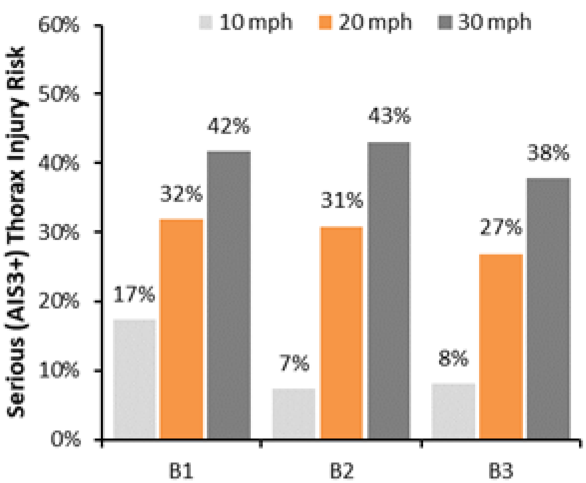

(b)

Fig. 7. Mean serious (AIS3+) injury risks, split by impact speed, for the (a) head and (b) thorax for impacts between the three bus designs (B1, B2 and B3) and a 50th percentile male pedestrian across all impact positions.

The maximum percentage serious (AIS3+) head and thorax injury risk simulated for each bus front end design when impacting the 50th percentile male pedestrian model at each impact speed are illustrated in Figure 8. In general, the trend in this relationship is consistent with that of the mean serious head and thorax injury risks (as in Figure 7). The exception to this is the maximum B1 serious thorax injury risks observed at 20 mph and 30 mph are lower than the equivalent maximum thorax injury risks for the B2 and B3 bus front end designs, whilst the mean serious thorax injury risks were the highest for the B1 bus front end design. Maximum head injury risks at the 30 mph impact speed were observed when the pedestrian model was impacted in position 5, whilst at the 20 mph and 10 mph impact speeds this was observed for position 5 for B1 and position 4 for both B2 and B3. Maximum thorax injury risks at all speeds were observed when the pedestrian model was impacted in position 4 for B1 and position 5 for B2 and B3.

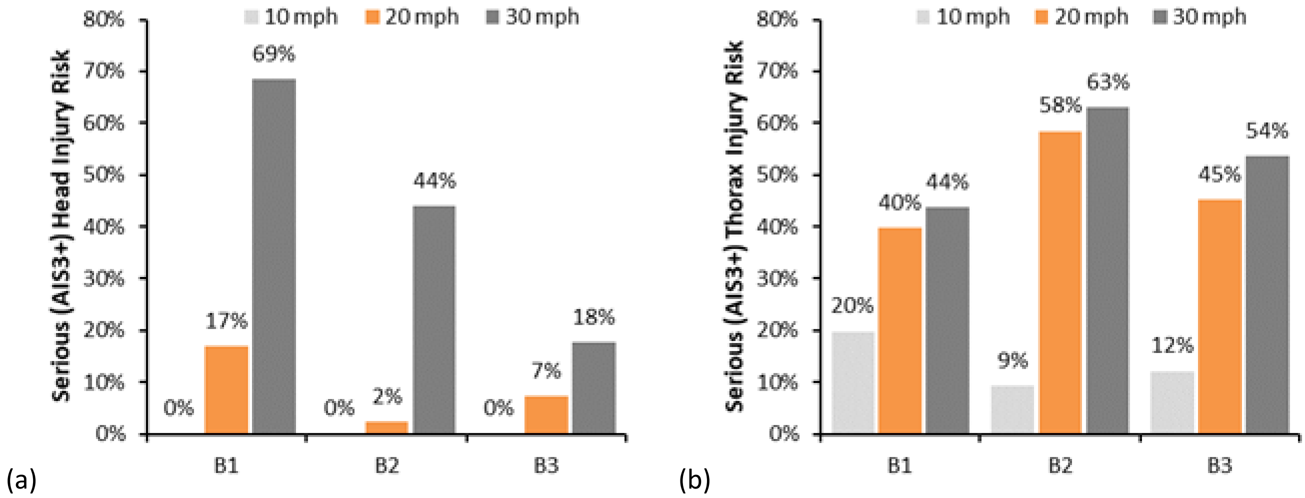

Fig. 8. Maximum serious (AIS3+) injury risks, split by impact speed, for the (a) head and (b) thorax for impacts between the three bus designs (B1, B2 and B3) and a 50th percentile male pedestrian across all impact positions.

Run-over results for collision between the three different bus designs and the 50th percentile male dummy for all impact positions and impact speeds is shown in Table 4. This data shows an improvement in run-over risk with each generation of bus front end design. Six (40%) of the fifteen scenarios would result in a run-over for B1, four (27%) would result in run-overs for B2 and one (7%) would result in a run-over for B3. All three designs run-over the pedestrian when the impact occurs in position 3 at 30 mph. A larger proportion of the collisions at 30 mph result in a pedestrian run-over, whereas no run-overs occur in collisions at 10 mph.

TABLE 4

Run-over results for each impact position, speed and bus design for the 50th percentile male pedestrian

Impact Position	Speed (mph)	B1	B2	B3
1	10	-	-	-
2	10	-	-	-
3	10	-	-	-
4	10	-	-	-
5	10	-	-	-
1	20	-	-	-
2	20	Run-Over	Run-Over	-
3	20	-	-	-
4	20	-	-	-
5	20	-	-	-
1	30	Run-Over	Run-Over	-
2	30	Run-Over	Run-Over	-
3	30	Run-Over	Run-Over	Run-Over
4	30	Run-Over	-	-
5	30	Run-Over	-	-

IV. DISCUSSION

Summary of principle findings

This research investigated whether the global geometry of bus front ends can be enhanced to minimise head injury, thorax injury and run-over risks caused during pedestrian bus collisions. Through a Design of Experiments (DOE) approach, this research observed that, for a range of impact speeds and positions, pedestrian injury and run-over risks were minimised for a bus front end design with a vertical rake angle of 7°, a rake angle transition height of 753 mm and an inner and outer horizontal angle envelope of 16° and 24°. When compared to two existing bus front end designs (B1 and B2), this enhanced bus front end design (B3) improved average serious (AIS3+) head injury risks by 26-37 pp at impact speeds of 30 mph, average serious (AIS3+) thorax injury risks by 4-5 pp across impact speeds of 20 mph and 30 mph and run-over risks by 20-33 pp at all impact speeds. This research therefore indicates that substantial casualty saving benefits may be gained with greater consideration given to the global geometry of bus front end designs.

Discussion of findings

Although this research is the first to specifically investigate whether the global geometry of bus front ends may be enhanced to improve the outcomes of pedestrian collisions, the optimisation of front end designs has previously been evaluated within both the HGV and tram sectors [4,5,10,12]. Head injury risks in this research were reduced by 26-37 pp at impact speeds of 30 mph with the B3 bus front end design, whilst head injury risks at speeds of 20 mph and 10 mph were <6% for all bus designs. Previous research has found similar head injury risk reductions during primary impacts, with the 80 mm forward displacement of the front trim panel relative to the windscreen and angled windscreens reducing AIS3+ head injury risks for adults by >43 pp [12] and a series of padded underrun guards and energy absorbing front trim reducing adult AIS3+ head injury risks by >25% [10]. While a number of factors may exist to explain the reasons for this improved performance, the combination of the curvature and raking of the B3 bus front end design seemed to better interact with the pedestrian torso to reduce the number, and impact speed, of interactions between the head and bus windscreen or bodywork.

Serious thorax injuries were not as affected by bus front end design as head injuries were in this study, with only a 4-5 pp reduction in serious thorax injury risk observed at impact speeds of 20 mph and 30 mph for the B3 bus front end design. Although this improved performance may again be explained by a number of factors, the curvature and raking of the B3 bus front end design seemed to better interact with the torso of the pedestrian to more evenly distribute loading during impact. Toward the centre of the bus, the greater vertical rake angles and lower rake transition heights associated with the B3 bus front end design seemed to concurrently engage the pelvic, abdomen, thorax and shoulder regions for longer periods of the impact. This is in direct comparison to existing bus front end designs (in particular B1), which engaged the shoulder and thorax regions much earlier in the impact thus loading this region for a considerably longer period. Toward the edges of the bus, the greater horizontal curvature seemed to deflect the pedestrian laterally away from the bus, thus seemingly transferring less energy to the pedestrian torso during the impact.

Run-over risks were substantially affected by bus front end geometry, with the proportion of run-over events predicted for the B3 bus front end design estimated to be only 7% across all impact speeds, when compared to 40% and 27% for the B1 and B2 bus front end designs respectively. Previous research has observed similar run-over risk reductions, with optimised truck front end designs causing run-over events in <12.5% of collisions and standard truck front end designs running over a VRU in 66-83% of collisions across a range of VRU sizes, vehicle manoeuvres, gait cycles, impact angles and impact positions [4,5]. The single run-over event simulated for the B3 bus front end design in this study occurred at the highest impact speed (30 mph) and at position 3, the least horizontally angled part of the bus. It is clear that, during a collision, the flatter the bus front end surface is that a pedestrian impacts and the higher the bus impact speed, the greater the run-over risk.

Research impact

By enhancing the global geometry of the bus front end, this research observed that the risks of serious head injuries may be reduced by 26-37 pp at impact speeds of 30 mph, the risks of serious thorax injuries may be reduced by 4-5 pp at impact speeds of 20 mph and 30 mph and the risks of run-overs reduced by 20-33 pp at all impact speeds. This indicates that enhanced bus front end geometries may therefore be able to contribute to reducing the substantial number of fatally and seriously injured pedestrians involved in bus collisions each year.

To fully realise these casualty saving benefits however, local and national authorities must implement policies and legislation to encourage the future adoption of enhanced bus front end geometries. In London, a 'Vision Zero' approach to road casualties was set out in the Mayor of London's 2018 Transport Strategy [18]. It aims for no person to be killed in, or by, a London bus by 2030 and for the elimination of fatalities and serious injuries by 2041. The results of this study have since been used by Transport for London's Bus Safety Standard to specify mandatory requirements for a bus front end design envelope for all new buses from 2024 [19]. The adoption of enhanced bus front end designs was forecast to prevent 15-20 pedestrian deaths and 89-120 serious pedestrian injuries in London between 2019-2031 [13].

Research limitations and future research

Despite this being a detailed analysis of the kinematics of pedestrian collisions with a wide range of bus front end geometries, there remain a number of limitations to the scope of this study that require further research. A greater number of existing bus front end designs could have been modelled to improve understanding of the variation in the safety performance of bus front end designs both across and outside of the TfL bus fleet. This argument may also be extended to modelling a greater number of enhanced bus front end designs and, as such, care should be taken in extrapolating the results reported here to bus front end designs that differ significantly from those used in this study.

Only five impact points were investigated by this research and, as such, the pedestrian impact kinematics may have been influenced by local features. Although these five impact points covered the key regions of the bus front end, future research could perform a parametric sweep of pedestrian impact positions across the bus front end to better understand the effect of impact position on outcomes. Whilst pedestrian gait, travel direction and travel speed have been observed to effect outcomes [6,8,12], these parameters were not varied within this study and, as such, their influence on outcomes should be investigated further.

The biofidelity of the simulation could also be improved, with the use of a combined EuroSID-IIre thorax with a Hybrid III FAST model limiting the biofidelity of the VRU model. Whilst there are more biofidelic human body models that may have been used, a trade-off exists between simulation biofidelity and the computational costs of running more complex models. For this research, the biofidelic response of the shoulder-thorax response was considered the most critical to represent during a collision and so the decision to combine a EuroSID-IIre thorax with the fast Hybrid III model seemed to be a reasonable approach. As each simulation was run for only 250 ms to reduce the computational costs of the analysis, the kinematics of the pedestrian throw following this point in time was only estimated. Although these estimations were verified, future research could further evaluate the post-primary impact kinematics (including secondary impacts with the ground and run-over events).

It is also important to ensure that there are no unintended consequences for any particular road user group. This research primarily based its simulations on impacts between the 50th percentile male dummy and bus front ends, with safety performance assessed primarily for head injury, thorax injury and run-over risk. Injury risks for other road user groups, in particular 5th percentile females and cyclists, that maybe adversely affected by these proposed design requirements should also be investigated. Finally, the effect of vertically raking the front end of a bus on leg injury risk also remains unknown.

V. CONCLUSIONS

Enhanced bus front end designs may be implemented to reduce the severity of the head and thorax injuries sustained by a pedestrian in a collision with a bus, whilst also reducing the probability of the pedestrian being run-over by the bus following the collision. Through a computational simulation approach this research study established that, for a range of impact speeds and positions, pedestrian injury risks may be minimised for a bus front end design with a vertical rake angle of 7°, a rake angle transition height of 753 mm and inner and outer horizontal angles of 16° and 24°. This enhanced bus front end geometry was observed to provide improvements in average serious (AIS3+) head injury risks (26-37 pp at impact speeds of 30 mph), serious (AIS3+) thorax injury risks (4-5 pp at impact speeds of 20 mph and 30 mph) and run-over risks (20-33 pp across all impact speeds), when compared to existing bus front end designs. Adoption of enhanced bus front end designs therefore show substantial potential for improving bus collision injury outcomes for pedestrians, through the reduction of head injury, thorax injury and run-over risks. Future research is, however, required to further optimise this enhanced bus front end design for the collision parameters not investigated by this study (i.e. different pedestrian sizes), whilst changes in secondary impact injury risks should also be considered.

VI. ACKNOWLEDGEMENTS

The authors would like to acknowledge TfL for funding this research through their Bus Safety Standard (BSS) programme, as well as GRM Consulting Ltd for their modelling and simulation expertise.

VII. REFERENCES

[1] European Commission. (2018) Directorate General for Transport, *Traffic Safety Basic Facts on Heavy Goods Vehicles and Buses*, Brussels.

[2] Edwards, A *et al*. (2018) TRL Limited, *Analysis of bus collisions and identification of countermeasures (PPR819)*, Crowthorne.

[3] Seidl *et al*. (2017) European Commission, *In depth cost-effectiveness analysis of the identified measures and features regarding the way forward for EU vehicle safety*, Brussels.

[4] De Nooij, M *et al*. (2009) RWTH Aachen, *APROSYS SP 9: Final APROSYS report (AP-SP90-0008)*, Aachen.

[5] Welfers, T *et al*. (2011) Transport & Environment, *Design of a Tractor for Optimised Safety and Fuel Consumption*, Brussels.

[6] Hamacher, M *et al*. Modification of a truck front for improved kinematics in run over accidents, *21st International Technical Conference on the Enhanced Safety of Vehicles (ESV)*, 2009, Stuttgart, Germany.

[7] Robinson, B *et al*. (2010) TRL Limited, *Safer aerodynamic frontal structures for trucks: final report (PPR533)*, Crowthorne.

[8] Feist, F *et al*. Pedestrian collisions with flat-fronted vehicles injury patterns and importance of rotational accelerations as a predictor for traumatic brain injury (TBI), *21st International Technical Conference on the Enhanced Safety of Vehicles (ESV)*, 2009, Stuttgart, Germany.

[9] Martin, P *et al*. (2017) European Commission, *Study on enhanced truck front end designs (TFEDs): Safety benefits for vulnerable road users (VRUs): final report*, Brussels.

[10] Grzebieta R, Rechnitzer G. Tram Interface Crashworthiness, *Proceedings of the International Crashworthiness Conference – ICRASH*, 2000, Bolton, UK.

[11] Hyncik, L *et al*. (2008) Optimisation of tram face with respect to passive safety, *Applied and Computational Mechanics*, 2, 53-62.

[12] Weber, T *et al*. Optimising the Design of Tramways to Mitigate Injury Risk in Pedestrian Impacts, *IRCOBI Conference Proceedings*, 2015, Lyon, France.

[13] Martin, P *et al*. (2018) TRL Limited, *The Transport for London Bus Safety Standard: Vulnerable Road User (VRU) Frontal Crashworthiness*. Crowthorne.

[14] UN Regulation 127. *Uniform provisions concerning the approval of motor vehicles with regard to their pedestrian safety performance (Addendum 126)*, Geneva.

[15] Knight, I *et al*. (2018) TRL Limited, *The Transport for London Bus Safety Standard: Advanced Emergency Braking (AEB) (PPR932)*. Crowthorne.

[16] Crabtree, M *et al*. (2014) TRL Limited, *A review of pedestrian walking speeds and time needed to cross the road (PPR700)*, Crowthorne.

[17] Kuppa, S. Injury criteria for side impact dummies. National Transportation Biomechanics Research Center, NHTSA, 2004.

[18] Mayor of London (2018) Greater London Authority, *Mayor's Transport Strategy*, London.

[19] Transport for London (2018), Transport for London, *Bus Safety Standard: Executive Summary*, London.